

Crystallization and characteristics of {100}-oriented diamond with CH₄N₂S additive under high pressure and high temperature*

Yong Li(李勇)[†], Debing Tan(谭德斌), Qiang Wang(王强), Zhengguo Xiao(肖政国),
Changhai Tian(田昌海), and Lin Chen(陈琳)

Department of Physics and Electrical Engineering, Tongren University, Tongren 554300, China

(Received 6 May 2020; revised manuscript received 28 May 2020; accepted manuscript online 5 June 2020)

Diamond crystallization was carried out with CH₄N₂S additive in the FeNiCo-C system at pressure 6.0 GPa and temperature ranging from 1290 °C to 1300 °C. The crystallization qualities of the synthetic crystals were characterized by Raman spectra and the Raman peaks located at 1331 cm⁻¹. Fourier transform infrared (FTIR) results showed that the hydrogen-related absorption peak of the as-grown diamond was at 2920 cm⁻¹, respectively. Interestingly, A-center nitrogen was observed in the obtained diamond and the characteristic absorption peaks located at 1095 cm⁻¹ and 1282 cm⁻¹. Especially, the absorption peak at 1426 cm⁻¹ attributing to the aggregation B-center nitrogen defect was distinctly found when the CH₄N₂S content reached 0.3 mg in the synthesis system, which was extremely rare in synthetic diamond. Furthermore, optical color centers in the synthesized crystals were investigated by photoluminescence (PL).

Keywords: high pressure and high temperature, diamond, crystallization, characteristics

PACS: 92.60.hv, 81.05.ug, 81.10.-h, 61.72.jn

DOI: 10.1088/1674-1056/ab99b9

1. Introduction

Because of its extremely excellent performances, diamonds attract significant attention and are extensively used in various fields.^[1-7] Nitrogen impurity is the major impurity in natural diamonds, which can affect the properties of diamonds, especially optical properties.^[8,9] Almost all natural diamonds contain the aggregation A-center (pairs of nearest neighboring substitutional nitrogen) or B-center (four nitrogen atoms around a vacancy) nitrogen impurities. Additionally, natural diamonds are generated at a pressure of about 5–7 GPa and temperature ranging from 900 °C to 1200 °C in the Earth's mantle. The corresponding FTIR absorption peaks of A-center aggregation nitrogen impurity locate at 480 cm⁻¹, 1095 cm⁻¹, 1203 cm⁻¹, 1282 cm⁻¹, and 1693 cm⁻¹ in natural diamond.^[10,11] Sutherland *et al.* proposed in 1954 that the seven peaks for B-center nitrogen in natural diamond located at 328 cm⁻¹, 780 cm⁻¹, 1003 cm⁻¹, 1171 cm⁻¹, 1332 cm⁻¹, 1372 cm⁻¹, and 1426 cm⁻¹.^[10-12] Generally, the single substitutional nitrogen defect (C-center) exists in the synthetic diamond. A-center nitrogen can be obtained in diamond synthesized by the addition of nitrogenous compound into the synthesis system and the FTIR absorption of A-center nitrogen located at 1282 cm⁻¹.^[13-15] However, the corresponding absorption at 1095 cm⁻¹ for A-center in synthesized diamond is seldom reported. B-center nitrogen can be produced at 7 GPa and 1850 °C or by HPHT annealing treatment for an as-grown diamond at about 2000 °C.^[16] Additionally, the aggregation

nitrogen impurities also can be realized by low-pressure/high-temperature annealing.^[17] Presently, the genesis of natural diamonds has still remained elusive and needs further understanding. It is considered that nitrogen, hydrogen, and sulfur impurities co-exist in the natural diamond formation environment. In order to provide experimental references for the further study of the formation mechanism of natural diamond, the CH₄N₂S additive is added in the synthesis system during the diamond growth to simulate the formation of natural diamond.

In this study, we obtain A-center and B-center nitrogen impurities in the synthesized diamond crystals under the current synthesis conditions. Furthermore, the optical color centers in the synthesized diamonds are investigated. The color centers in diamond are potential candidates for the applications in biomarking and as the sensitive probes of magnetic fields or quantum environments.^[3,4]

2. Experimental description

Pyrophyllite blocks are supplied by Stasheng new materials co. LTD. Graphite with purity 99.9% and FeNiCo alloy are employed as carbon source and catalyst for diamond synthesis. Synthetic diamond crystal size about 0.8 mm is used as the seed crystal and {100} surface is selected as the initial growth surface. Additionally, CH₄N₂S with purity 99.5% is used as the additive. Then, 0.05 g Ti and 0.05 g Cu are simultaneously added into the synthesis system as nitrogen getter to remove the nitrogen impurity produced from the raw materi-

*Project supported by the National Natural Science Foundation of China (Grant No. 11604246), Natural Science Foundation of Guizhou Province Education Department of China (Grant Nos. KY2017053 and KY2018343), Natural Science Foundation of Guizhou Province Science and Technology Agency of China (Grant Nos. 20181163 and LH 20177311), and Outstanding Young Science and Technology Talents of Guizhou Province of China (Grant No. 20195673).

[†]Corresponding author. E-mail: likaiyong6@163.com

als. Synthesis pressure is calibrated through pressure-induced phase transitions of Bi, Tl, and Ba. Experimental temperature is measured by the Pt6%Rh–Pt30%RH thermocouple with a precision of ± 1.5 °C.

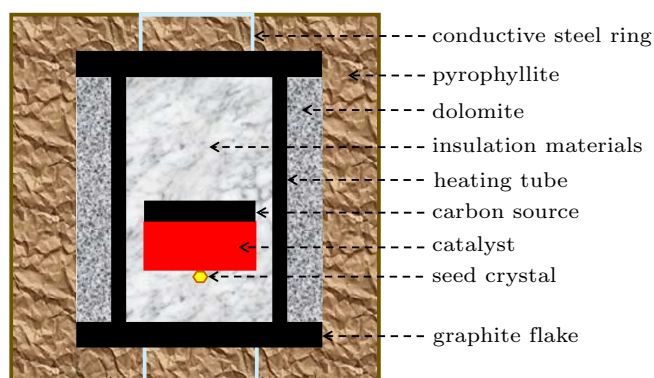


Fig. 1. Schematic diagram of the cell for diamond synthesis.

In this study, the synthesis experiments are carried out in a China-type large volume cubic high-pressure apparatus, using a temperature gradient growth (TGG) method, and the schematic diagram of the cell for diamond synthesis is shown in Fig. 1. The crystal growth principle is described as following. The highest temperature of the heating tube locates at the middle position when it heats, and the temperature decreases gradually along the vertical axis. Therefore, the temperature gradient generates between the carbon source and the seed crystal. Carbon dissolved into the catalyst at a high-temperature region will be transported to the vicinity of the seed crystal by the temperature gradient as the driving force. Then, the transported carbon will crystallize on the seed crystal to achieve the epitaxial growth of the diamond.

After the HPHT treatment, the diamond sample is placed in a boiling dilute HNO_3 until the diamond completely detaches from the FeNiCo catalyst. Then, the sample is boiled in the $\text{HNO}_3 + \text{HSO}_4$ mixture to clean up the residuum on the diamond surfaces. Next, the diamond samples are cleaned with ultrasound in anhydrous ethanol. Later, the typical crystals are characterized by Raman, FTIR, and PL spectra, respectively.

3. Results and discussion

Diamonds crystallization on {100}-oriented seeds was conducted at pressure 6.0 GPa and temperature ranging from 1290 °C to 1300 °C via the TGG method and the experimental parameters are summarized in Table 1. Generally, the morphology of synthetic diamond crystal sensitively depended on the temperature condition and was significantly affected by the involved impurities in the diamond during the crystallization process. It was clearly seen from Fig. 2 that all the produced diamond crystals exhibited cub-octahedral morphologies, which were mainly composed of {100} and {111}

surfaces with some high-index crystal surfaces ({311}, etc.). As is well known, synthetic diamond always displayed typical yellow resulting from the single substitutional nitrogen impurity (C-center), defined as Ib type diamond. As illustrated in Figs. 2(a) and 2(b), the obtained diamond crystals displayed a yellow color, indicating that the two samples should contain C-center nitrogen defect in crystal lattices. However, the synthesized diamond (Figs. 2(c) and 2(d)) exhibited colorless because of the addition of Ti/Cu as nitrogen getter additive in the synthesis system. Additionally, the visible defect on the top {100} surface of the crystal (Fig. 2(d)) was found when the addition content of $\text{CH}_2\text{N}_2\text{S}$ reached 0.3 mg.

Table 1. Experimental parameters of diamond synthesized in the FeNiCo-C system.

Run	$\text{CH}_4\text{N}_2\text{S}/\text{mg}$	Ti/Cu	Temperature/°C	Time/h
a	0.2	0	1295	21
b	0.3	0	1290	21
c	0.2	0.05 gTi/0.05 gCu	1295	21
d	0.3	0.05 gTi/0.05 gCu	1300	21

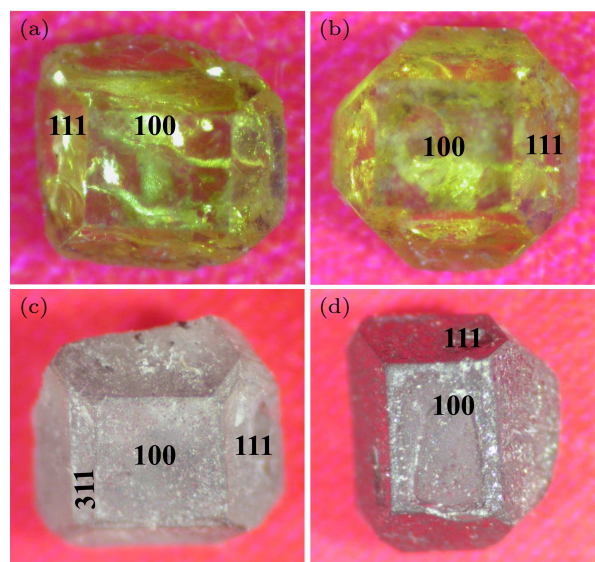


Fig. 2. Optical morphology of the synthesized diamond crystals with different concentrations of $\text{CH}_4\text{N}_2\text{S}$ additive or $\text{CH}_4\text{N}_2\text{S} + \text{Ti/Cu}$ additives. (a) 0.2 mg $\text{CH}_4\text{N}_2\text{S}$ additive, (b) 0.3 mg $\text{CH}_4\text{N}_2\text{S}$ additive, (c) 0.2 mg $\text{CH}_4\text{N}_2\text{S} + \text{Ti/Cu}$ additives, (d) 0.3 mg $\text{CH}_4\text{N}_2\text{S} + \text{Ti/Cu}$ additives.

Generally, the typical Raman peak of diamond with sp^3 hybrid located at 1332 cm^{-1} . As shown in Fig. 3, the characteristic peaks shifted to 1331 cm^{-1} (first-order longitudinal phonon) with straight background lines, meaning that the characteristic peaks were probably affected by the impurities involved in diamond structure. Additionally, the Raman peaks centered at 1343 cm^{-1} (D peak) and the posterior peak locating at 1560 cm^{-1} for graphitic carbon (G peak) resulting from the graphite sp^2 hybrid bond structure were not observed.^[18] It indicated that diamond was the only phase with a sp^3 hybrid structure. The full width at half maximum (FWHM) for the perfect diamond crystal should be zero, where carbon

atoms strictly arranged according to spatial lattices. However, FWHM for the synthesized diamond exhibited specific values, resulting from that the lattice orientation was not exactly the same and the incorporation of impurity defects into the diamond structure. Therefore, the crystallization quality of the synthesized diamond could be characterized by the corresponding FWHM. In this work, the FWHM values were obtained using the Lorentz fit and displayed in Fig. 3. On the whole, the FWHM values corresponding to the synthesized crystals became wider with the content of $\text{CH}_4\text{N}_2\text{S}$ increasing in the synthetic system. It indicated that more defects generated with the content of $\text{CH}_4\text{N}_2\text{S}$ increasing in the synthetic system.

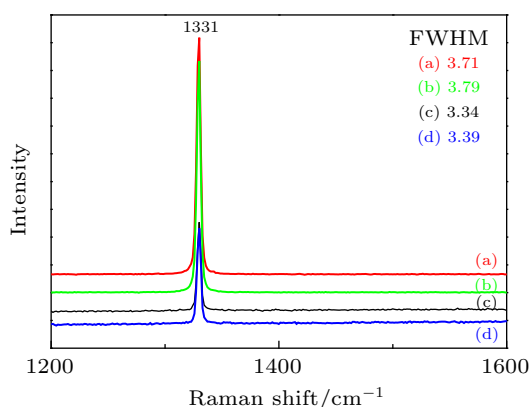


Fig. 3. Raman shift and FWHM of the synthesized diamond with different concentrations of $\text{CH}_4\text{N}_2\text{S}$ additive or $\text{CH}_4\text{N}_2\text{S} + \text{Ti/Cu}$ additives. (a) 0.2 mg $\text{CH}_4\text{N}_2\text{S}$ additive, (b) 0.3 mg $\text{CH}_4\text{N}_2\text{S}$ additive, (c) 0.2 mg $\text{CH}_4\text{N}_2\text{S} + \text{Ti/Cu}$ additives, (d) 0.3 mg $\text{CH}_4\text{N}_2\text{S} + \text{Ti/Cu}$ additives.

FTIR was a useful scatheless technique for distinguishing impurities and their states in the diamond crystal. Figure 4 recorded the FTIR spectra of the synthesized diamonds with $\text{CH}_4\text{N}_2\text{S}$ additive under the HPHT conditions, which could be divided into three zones. The wavenumber of the one-phonon zone was below 1330 cm^{-1} . Then, the two-phonon zone occupied between 1332 cm^{-1} and 2667 cm^{-1} in the FTIR spectrum. In addition, the three-phonon zone located at range from 2667 cm^{-1} to 3996 cm^{-1} . In Fig. 4(a) inset, the absorption peaks locating at 2800 cm^{-1} and 2920 cm^{-1} were noticed in red and black curves, resulting from boron introduced by unconsciousness and C–H vibrations, respectively.^[19,20] Furthermore, it clearly showed that the absorption intensity of 2800 cm^{-1} peak was apparently stronger than that of 2920 cm^{-1} peak. However, the characteristic peaks 2800 cm^{-1} and 2920 cm^{-1} were absent in green and blue curves. As revealed in Fig. 4(b), the weak peaks at 847 cm^{-1} attributing to sulfur impurity in green and blue curves were found, indicating that sulfur was incorporated into the diamond crystal. The nitrogen impurities were found in green and blue curves in the produced diamond in the form of C-center with strong absorption peaks at 1130 cm^{-1} and 1344 cm^{-1} . Additionally, we noticed a broad shoulder at 1282 cm^{-1} for

A-center nitrogen impurity in green and blue curves, indicating that the two synthesized crystals contained both C-center and A-center nitrogen defects. The characteristic peaks at 1130 cm^{-1} and 1344 cm^{-1} for C-center were absent in the sample with 0.2 mg/0.3 mg $\text{CH}_4\text{N}_2\text{S} + \text{Ti/Cu}$ additives, marked by red/black curve, showing that the corresponding crystals did not contain C-center nitrogen. However, the absorption locating at 1095 cm^{-1} confirmed that A-center nitrogen existed in these two diamonds, although there was no absorption signal at about 1282 cm^{-1} .^[10–12,15] It probably signifies that Ti/Cu only could remove the nitrogen in the free state in the synthesis system, but the nitrogen impurities in the complex form in the synthesis system cannot be removed. Combining with previous reports, A-center nitrogen locating at 1282 cm^{-1} tended to generated when the concentration of the free nitrogen was high in the synthesis system.^[14,15,21] Also, although A-center nitrogen could be obtained in a low nitrogen concentration system, its synthesis temperature condition reached about $1600\text{ }^\circ\text{C}$ – $1850\text{ }^\circ\text{C}$, even to produce B-center nitrogen at about $2000\text{ }^\circ\text{C}$ by the HPHT annealing treatment.^[16,22] It was considered that the higher temperature played the vitally important role in promoting the transformation of C-center nitrogen to A-center or B-center nitrogen aggregation. Under the current synthesis conditions ranging from $1290\text{ }^\circ\text{C}$ to $1300\text{ }^\circ\text{C}$, it was not obviously enough to convert the C-center nitrogen into the aggregation states in the diamond. Basing on what had been discussed above, we speculated that the formation of the A-center nitrogen at 1282 cm^{-1} was related to the free nitrogen concentration in the synthesis system. However, the formation of A-center nitrogen locating at 1095 cm^{-1} associated with the structure of the $\text{CH}_4\text{N}_2\text{S}$ additive, which contained $-\text{N}-\text{C}-\text{N}-$ chemical structure. The $-\text{N}-\text{C}-\text{N}-$ structure probably transformed $-\text{C}-\text{N}-\text{N}-$ structure (A-center nitrogen) by the assistance role of the vacancy defect, which was removable as the system temperature above $700\text{ }^\circ\text{C}$.^[23] Furthermore, A-center nitrogen migration may be affected by the removable vacancy to form B-center nitrogen defects,^[24] which needed to further understanding. However, the corresponding absorption at 847 cm^{-1} was not observed in green and blue curves. According to the FTIR data results, the sulfur element was only present in diamonds, containing C-center nitrogen impurity. It allowed us to infer that the incorporation of the sulfur element was closely related to C-center nitrogen impurity in the diamond. It was consistent with the previous report that the entry of sulfur impurity into IIa type diamond was prohibited, which did not contain C-center N impurity.^[25]

In Fig. 5, PL peak at 488 nm was produced 488 nm laser and the sharp feature at 522 nm was common for the diamond, respectively.^[23] In Fig. 5(a), a shoulder locating at 503 nm was noticed, which was responsible for the H3 color center (N–V–

N).^[26] When the $\text{CH}_4\text{N}_2\text{S}$ amount was 0.3 mg in the synthesis system, PL peaks at 554.7 nm and 637 nm were found, which were the nitrogen-bearing color center and NV^- color center, respectively.^[27,28] Since neither Fig. 5(c) nor Fig. 5(d) contained C-center nitrogen impurity, the NV color center was not observed. However, the Ni-related characteristic peaks at 695 nm and 793.6 nm were established.^[27,29] Especially, 793.6 nm corresponding to NE8 color center may have more potential applications than the common NV centers, but also benefited to design a practical diamond color center-based single-photon source.

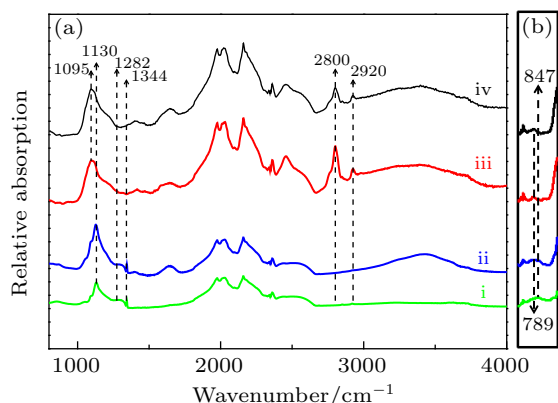


Fig. 4. (a), (b) FTIR spectra of the synthesized diamond crystals with different concentrations of $\text{CH}_4\text{N}_2\text{S}$ additive or $\text{CH}_4\text{N}_2\text{S}$ + Ti/Cu additives. The green, blue, red, and black curves represent the FTIR spectra of the synthesized diamond crystals with 0.2 mg $\text{CH}_4\text{N}_2\text{S}$ additive, 0.3 mg $\text{CH}_4\text{N}_2\text{S}$ additive, 0.2 mg $\text{CH}_4\text{N}_2\text{S}$ + Ti/Cu additives, and 0.3 mg $\text{CH}_4\text{N}_2\text{S}$ + Ti/Cu additives, respectively.

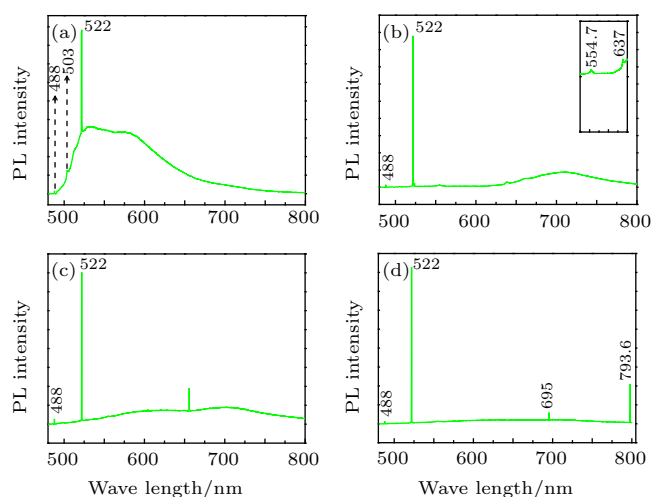


Fig. 5. PL spectra of the synthesized diamond crystals taken at room temperature, excited by the 488 nm line: (a) with 0.2 mg $\text{CH}_4\text{N}_2\text{S}$ additive, (b) with 0.3 mg $\text{CH}_4\text{N}_2\text{S}$ additive, (c) with 0.2 mg $\text{CH}_4\text{N}_2\text{S}$ + Ti/Cu additives, (d) with 0.3 mg $\text{CH}_4\text{N}_2\text{S}$ + Ti/Cu additives.

4. Conclusion

Diamond crystals with $\{100\}$ -oriented were synthesized with $\text{CH}_4\text{N}_2\text{S}$ additive under the HPHT conditions, exhibiting yellow or colorless. Raman peaks of the crystalline diamonds only showed one sharp peak at 1331 cm^{-1} without sp^2 hybrid phases. Hydrogen element was incorporated into diamond lattices and the FTIR peaks located at 2920 cm^{-1} . The FTIR

absorption peak located at 1095 cm^{-1} and 1282 cm^{-1} in the synthesized diamond, resulting from A-center nitrogen impurity. More importantly, the rare B-center nitrogen defect was observed in the diamond synthesized with 0.3 mg $\text{CH}_4\text{N}_2\text{S}$ addition in the synthesis system. Furthermore, H3, NV^- , and NE8 color centers were acquired in current synthesis conditions without annealing treatment.

References

- [1] Guo M M, Li S S, Hu M H, Su T C, Wang J Z, Gao G J, You Y and Nie Y 2020 *Chin. Phys. B* **29** 018101
- [2] Li Y, Li Y D, Wang Y, Zhang J, Song M S, She Y C and Chen X Z 2018 *Cryst. Eng. Comm.* **20** 4127
- [3] Angerer A, Streltsov K, Astner T, Putz S, Sumiya H, Onoda S, Isoya J, Munro W J, Nemoto K, Schmiedmayer J and Majer J 2018 *Nat. Phys.* **14** 1168
- [4] Dutt M V G, Childress L, Jiang L, Togan E, Maze J, Jelezko F, Zibrov A S, Hemmer P R and Lukin M D 2007 *Science* **316** 1312
- [5] Maze J R, Stanwix P L, Hodges J S, Hong S, Taylor J M, Cappellaro P, Jiang L, Zibrov A S, Yacoby A, Walsworth R L and Lukin M D 2008 *Nature* **455** 644
- [6] Zhang J F, Yang P Z, Ren Z Y, Zhang J C, Xu S R, Zhang C F, Xu L and Hao Y 2018 *Acta Phys. Sin.* **67** 068101 (in Chinese)
- [7] Xu H, Liu J J, Ye H T, Coathup D J, Khomich A V and Hu X J 2018 *Chin. Phys. B* **27** 096104
- [8] Hu M H, Bi N, Li S S, Su T C, Hu Q, Jia X P and Ma H A 2015 *Chin. Phys. B* **24** 038101
- [9] Wang J Z, Li S S, Hu M H, Su T C, Gao G J, Guo M M, You Y and Nie Y 2020 *Int. J. Refract. Met. Hard Mater.* **87** 105150
- [10] Briddon P R and Jones R 1993 *Physica B* **185** 179
- [11] Salustro S, Ferrari A M, Gentile F S, Denmarais J K and Rérat M 2018 *J. Phys. Chem. A* **122** 594
- [12] Sutherland G B B M, Blackwell D E and Simeral W G 1954 *Nature* **174** 901
- [13] Li Y, Jia X P, Hu M H, Yan B M, Zhou Z X, Fang C, Zhang Z F and Ma H A 2012 *Int. J. Refract. Met. Hard Mater.* **34** 27
- [14] Guo L S, Ma H A, Chen L C, Chen N, Miao X Y, Wang Y, Fang S, Yang Z Q, Fang C and Jia X P 2018 *Cryst. Eng. Comm.* **20** 5457
- [15] Li Y, Jia X P, Yan B M, Zhou Z X, Fang C, Zhang Z F, Sun S S and Ma H A 2012 *Journal of Crystal Growth* **359** 49
- [16] Pal'yanov Y N, Kupriyanov I N, Borzdov Y M, Sokol A G and Khokhryakov A F 2009 *Cryst. Growth Des.* **9** 2922
- [17] Meng Y F, Yan C S, Lai J, Krasnicki S, Shu H Y, Yu T, Liang Q, Mao H K and Hemley Russell J 2008 *Proc. Acad. Natl. Sci. USA* **105** 17620
- [18] Akaishi M, Handa H, Sato Y, Setaka N, Ohsawa T and Fukunaga O 1982 *J. Mater. Sci.* **17** 193
- [19] Fuchs F, Wild C, Schwarz K and Koidl P 1995 *Diam. Relat. Mater.* **4** 652
- [20] Li Y, Jia X P, Hu M H, Liu X B, Yan B M, Zhou Z X, Zhang Z F and Ma H A 2012 *Chin. Phys. B* **21** 058101
- [21] Huang G F, Jia X P, Yin J W, Ma H A and Zheng Y J 2013 *Int. J. Refractory Metals and Hard Mater* **41** 517
- [22] Liu X B, Jia X P, Fang C and Ma H A 2016 *Cryst. Eng. Comm.* **18** 8506
- [23] Chen N, Ma H A, Yan B M, Chen L C, Chen L X, Guo L S, Miao X Y, Fang C and Jia X P 2018 *Cryst. Growth Des.* **18** 3870
- [24] Mainwood A 1994 *Phys. Rev. B* **49** 7934
- [25] Li Y, Li S S, She Y C and Guan X M 2017 *Journal of Synthetic Crystals* **46** 778 (in Chinese)
- [26] Lindblom J, Hölsä J, Papunen H and Häkkinen H 2005 *American Mineralogist* **90** 428
- [27] Stanwix P L, Pham L M, Maze J R, Le Sage D, Yeung T K, Cappellaro P, Hemmer P R, Yacoby, Lukin M D and Walsworth R L 2010 *Phys. Rev. B* **82** 201201
- [28] Chen L C, Miao X Y, Ma H A, Guo L S, Wang Z K, Yang Z Q, Fang C and Jia X P 2018 *Cryst. Eng. Comm.* **20** 7164
- [29] Rabeau J R, Chin Y L, Praver S, Jelezko F, Gaebel T and Wrachtrup J 2005 *Appl. Phys. Lett.* **86** 131926